

AD-A086 723

AERONAUTICAL RESEARCH LABS MELBOURNE (AUSTRALIA)

F/6 11/6

FATIGUE-CRACK GROWTH IN D6AC STEEL HEAT-TREATED TO DIFFERENT VA--ETC (1)

APR 79 N E RYAN

UNCLASSIFIED

ARL/MAT-110

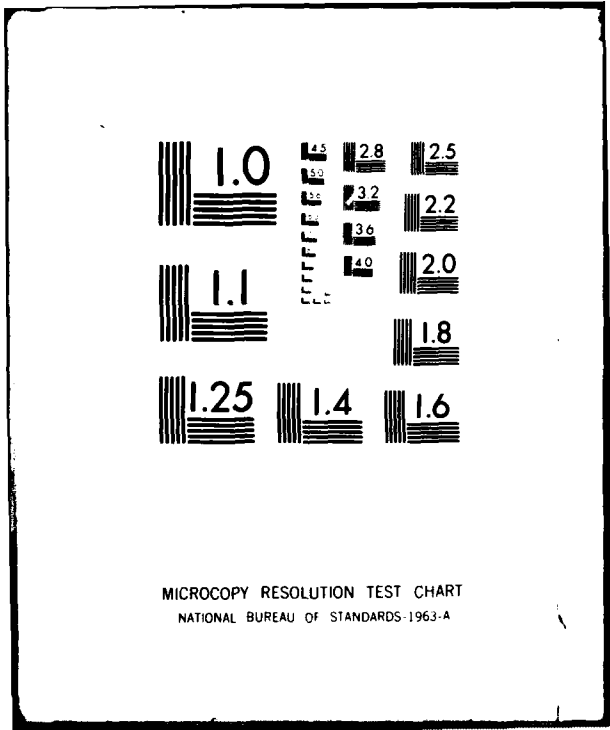
NL

1 of 1

25.94



END
DATE
FILMED
8-80
DTIC



MICROCOPY RESOLUTION TEST CHART
NATIONAL BUREAU OF STANDARDS-1963-A

LEVEL

12
P.S.



AD A 086723

DEPARTMENT OF DEFENCE
DEFENCE SCIENCE AND TECHNOLOGY ORGANISATION
✓ AERONAUTICAL RESEARCH LABORATORIES

MELBOURNE, VICTORIA

MATERIALS REPORT 110

DTIC
ELECTED
JUL 14 1980
S **C**

FATIGUE-CRACK GROWTH IN D6AC STEEL
HEAT-TREATED TO DIFFERENT VALUES
OF FRACTURE TOUGHNESS

by

N. E. RYAN

THE UNITED STATES NATIONAL
TECHNICAL INFORMATION SERVICE
IS AUTHORISED TO
REPRODUCE AND SELL THIS REPORT

Approved for Public Release.



© COMMONWEALTH OF AUSTRALIA 1979

DDC FILE COPY

COPY No **11**

APRIL 1979

80 7 11 005

12

AR-001-734

DEPARTMENT OF DEFENCE
DEFENCE SCIENCE AND TECHNOLOGY ORGANISATION
AERONAUTICAL RESEARCH LABORATORIES

14, ART/1117-118

MATERIALS REPORT 110

6

**FATIGUE-CRACK GROWTH IN D6AC STEEL
HEAT-TREATED TO DIFFERENT VALUES
OF FRACTURE TOUGHNESS**

by
N. E. RYAN



11) Apr 79

221

0.7K sub IC,

SUMMARY

Measurements of fatigue-crack growth in D6AC steel, heat-treated to various fracture-toughness levels, show that, under conditions where the growth mechanism produces striation markings and the crack extension per cycle is a linear function of a power of the stress intensity range, the rate of fatigue-crack growth is independent of fracture-toughness. At peak stress intensity values greater than 0.7 K_{IC}, the rate of growth accelerates as the critical stress intensity is approached and tensile modes of crack extension occur. At peak stress intensity values less than 18 MPa (m)^{1/2}, fractographic examination indicates a change in mechanism as the crack extension per cycle decreases more rapidly with decreasing peak stress intensity, approaching a threshold value of stress intensity dependent upon heat-treatment.

(S2014 rch
00 m)

The implications of these results for the choice of materials for service applications are discussed.



POSTAL ADDRESS: Chief Superintendent, Aeronautical Research Laboratories,
Box 4331, P.O., Melbourne, Victoria, 3001, Australia.

008650

This document has been approved for public release and sale; its distribution is unlimited.

AT

DOCUMENT CONTROL DATA SHEET

Security classification of this page: Unclassified

<p>1. Document Numbers</p> <p>(a) AR Number: AR-001-734</p> <p>(b) Document Series and Number: Materials Report 110</p> <p>(c) Report Number: ARL-Mat-Report-110</p>	<p>2. Security Classification</p> <p>(a) Complete document: Unclassified</p> <p>(b) Title in isolation: Unclassified</p> <p>(c) Summary in isolation: Unclassified</p>								
<p>3. Title: FATIGUE-CRACK GROWTH IN D6AC STEEL HEAT-TREATED TO DIFFERENT VALUES OF FRACTURE TOUGHNESS</p>									
<p>4. Personal Author(s): N. E. Ryan</p>	<p>5. Document Date: April, 1979</p>								
<p>6. Type of Report and Period Covered:</p>									
<p>7. Corporate Author(s):</p>	<p>8. Reference Numbers</p> <p>(a) Task: Air 72/8</p> <p>(b) Sponsoring Agency:</p>								
<p>9. Cost Code: 35 1610</p>									
<p>10. Imprint:</p>	<p>11. Computer Program(s) (Title(s) and language(s)):</p>								
<p>12. Release Limitations (of the document) Approved for public release</p>									
<p>12-0. Overseas:</p>	<table border="1" style="margin-left: auto; margin-right: auto;"> <tr> <td style="width: 20px;">N.O.</td> <td style="width: 20px;">P.R.</td> <td style="width: 20px;">I</td> <td style="width: 20px;">A</td> <td style="width: 20px;">B</td> <td style="width: 20px;">C</td> <td style="width: 20px;">D</td> <td style="width: 20px;">E</td> </tr> </table>	N.O.	P.R.	I	A	B	C	D	E
N.O.	P.R.	I	A	B	C	D	E		
<p>13. Announcement Limitations (of the information on this page): No Limitation</p>									
<p>14. Descriptors:</p> <p>Fatigue (materials) Steels Crack propagation</p>	<p>15. Cosati Codes:</p> <p>1106 2012</p>								
<p>14. Descriptors:</p> <p>Fractography Fractures (materials) Fracture strength</p>									

16.

ABSTRACT

Measurements of fatigue-crack growth in D6AC steel, heat-treated to various fracture-toughness levels, show that, under conditions where the growth mechanism produces striation markings and the crack extension per cycle is a linear function of a power of the stress intensity range, the rate of fatigue-crack growth is independent of fracture-toughness. At peak stress intensity values greater than 0.7 K_{IC}, the rate of growth accelerates as the critical stress intensity is approached and tensile modes of crack extension occur. At peak stress intensity values less than 18 MPa m^{1/2}, fractographic examination indicates a change in mechanism as the crack extension per cycle decreases more rapidly with decreasing peak stress intensity, approaching a threshold value of stress intensity dependent upon heat-treatment.

The implications of these results for the choice of materials for service applications are discussed.

CONTENTS

	Page No.
1. INTRODUCTION	1
2. EXPERIMENTAL	1
2.1 Steel Composition	1
2.2 Test Specimens and Heat Treatment	2
2.3 Mechanical Properties	2
2.4 Fatigue Tests	3
2.4.1 Pre-cracking	3
2.4.2 Test Atmosphere	3
2.4.3 Testing Procedures	3
2.4.4 Crack-Growth Measurements	3
2.5 Fractography by Electron Microscopy	3
3. EXPERIMENTAL OBSERVATIONS	3
3.1 Rate of Growth of Fatigue Cracks	3
3.2 Fractographic Examination	4
3.2.1 High Toughness Steel	4
3.2.2 Low Toughness Steel	4
3.2.3 High Strength, Medium Toughness Steel	5
4. DISCUSSION	5
5. CONCLUSIONS	6
REFERENCES	
FIGURES	
DISTRIBUTION	

Accession For	
NTIS OSA&I	<input checked="" type="checkbox"/>
DDC TAB	<input type="checkbox"/>
Unannounced Justification	
By _____	
Distributor/	
Availability Codes	
Dist	Avail and/or special
A	

1. INTRODUCTION

Linear-elastic fracture mechanics, with its concept of a stress-intensity factor $K\alpha\sigma_0a^{1/2}$ (where a = length of a pre-existing crack and σ_0 = the stress applied remote from the crack), provides a basis for the quantitative analysis of various crack-growth and fracture processes. The maximum, or critical, stress intensity factor, K_{1C} of a material relates to the onset of *unstable* crack growth to fracture and thus measures "fracture toughness". Sub-critical values of the stress intensity provide a measure of the mechanical 'driving force' for *stable* (sub-critical) crack-growth processes.

Fatigue cracking is a stable crack-growth process whose rate, according to Paris and Erdogan¹, can be represented by the relationship

$$da/dN = C\Delta K^m$$

where

da/dN is the crack extension per cycle

ΔK = the cyclic amplitude of stress intensity, $K_{\max} - K_{\min}$

C a material constant and m an exponent ≈ 4 .

Experimentally determined values of m commonly lie between 2 and 4 although values up to 8 have often been noted; wide variations in C are also obtained²⁻⁶. Factors influencing the values of C and m have received considerable attention over the past decade in the hope of formulating laws for predicting rates of fatigue-crack growth. The physical processes contributing to fatigue-crack extension are, however, not clearly understood and a number of theoretical expressions for fatigue-crack growth have been derived from bulk physical and mechanical properties, e.g. elastic modulus E , proof or yield stress σ_y , ultimate strength σ_U , fracture toughness K_{1C} and/or fracture strain ϵ_F . Good reviews of the various fatigue crack-growth laws have been given by Pelloux⁷ and Schwalbe⁸. Theoretical studies, in general, have concentrated on producing expressions to fit simple growth-rate relationships of the Paris-Erdogan form. Meanwhile, more careful experimental studies have shown that the relationship between fatigue crack-growth rate and ΔK cannot be attributed to one single mechanism. Departure from a simple power law was noted by Liu⁹ in 1964. Current analyses show that the relation between $\log da/dN$ and $\log \Delta K$ is a sigmoidal curve with three characteristic regions^{10,11,12}:

- (i) a region, corresponding to low growth rates and low ΔK , where a 'fatigue-threshold' cyclic stress intensity factor (K_{th}) is approached below which cracks might be considered as non-propagating,
- (ii) a central region where the linear relationship between $\log da/dN$ and $\log \Delta K$ is maintained, and
- (iii) a region where the rate of growth accelerates as the ΔK or K_{\max} value approaches K_{1C} .

In the work described here, the fatigue-crack growth rates in D6AC steel, heat-treated to produce a variety of mechanical properties have been examined. Particular attention was given to the influence of fracture toughness, since recent studies^{13,14} have shown that the fracture toughness could be varied (by different heat-treatment schedules), from 40 to 105 MPa.m^{1/2} without significantly changing the tensile properties.

2. EXPERIMENTAL

2.1 Steel Composition

D6AC steel manufactured to specification AMS6438 had the following chemical composition.

C	Mn	Si	P	S	Cr	Ni	Mo	V	Fe
0.44	0.75	0.22	0.004	0.002	1.08	0.7	1.0	0.1	rem. wt %

2.2 Test Specimens and Heat Treatment

Standard tensile and ASTM. T_2 , 19 mm thick, compact-tension, fracture-toughness specimens were machined from a single batch of 32 mm thick bar and heat-treated to four different schedules:

- A. Austenitize 930°C
Intermediate 'Ausbay' quench 520°C
Oil Quench
Double temper at 550°C
- B. Austenitize 930°C
Intermediate 'Ausbay' quench 520°C
Salt Quench 210°C
Double temper at 550°C
- C. Austenitize 930°C
Intermediate 'Ausbay' quench 520°C
Air cool
Double temper at 550°C
- D. Austenitize 930°C
Intermediate 'Ausbay' quench 520°C
Oil Quench
Double temper at 290°C.

2.3 Mechanical Properties

The mechanical properties, resulting from the above heat-treatments, are given in Table 1.

TABLE 1

Heat Treatment Schedule	Yield Strength 0.1% Proof MPa	Ultimate Tensile Strength MPa	Reduction in Area %	Elongation %	Fracture Toughness K_{Ic} MPa. $m^{1/2}$
A	1434-1454	1600-1620	47-51	14-17	98-105
B	1440-1460	1600-1630	48-51	14-17	78-86
C	1450-1470	1630-1650	44-48	13-15	42-48
D	1510-1518	1850-1910	32-35	11-12	54-60

Heat-treatments A, B and C gave essentially the same tensile strength properties but different toughness values, while heat-treatment D gave higher tensile properties and a medium fracture toughness level.

2.4 Fatigue Tests

2.4.1 Pre-cracking

Initial pre-cracks, about 3 mm long, were introduced into the compact-tension specimens prior to tests to determine toughness and fatigue crack-growth rates. The final extension of these pre-cracks was made with a cyclic K_{\max} of $\sim 15 \text{ MPa}\cdot\text{m}^{1/2}$ applied for 5 to 10×10^4 cycles.

2.4.2 Test Atmosphere

A constant environment was preserved by maintaining a flow of medically dry air ($\sim 0.5 \text{ mg/litre H}_2\text{O}$) through a Perspex box surrounding the test specimens.

2.4.3 Testing Procedures

With the exception of a few tests at amplitudes of stress intensity less than $15 \text{ MPa}\cdot\text{m}^{1/2}$, all fatigue tests were carried out at approximately 3 Hz using a variable-speed, eccentric-driven, fatigue machine which applied sine wave tension-tension loading. Tests at values of K_{\max} less than $15 \text{ MPa}\cdot\text{m}^{1/2}$ were carried out in an Amsler 'Vibrophone' machine at approximately 100 Hz. The applied cyclic amplitudes of stress intensity, ΔK , were essentially equal to K_{\max} as only a low K_{\min} was used (simply to maintain specimen alignment). Little, if any, mean load effects were introduced as the stress ratio ($R = K_{\min}/K_{\max}$) was always much less than 0.1.

2.4.4 Crack-Growth Measurements

Fatigue-crack extension was monitored during tests by observing the polished specimen surface through a microscope with a $\times 20$ graduated eyepiece. Crack-growth rates determined in this manner were later checked against other values determined fractographically. These quantitative fractographic measurements were facilitated by producing periodic "markers" on the fracture surface by changing the load level. Markers produced by decreasing the load level, by as much as 50 percent, and increasing the cyclic frequency from 3 to 20 Hz for 10,000 cycles, produced distinct bands (up to 0.3 mm wide) on the fracture surface. When the load levels were increased, by more than 20 percent, characteristic 'tide' markings were apparent on the fracture surfaces. Measurements of these progression marking were made using a profile-projecting, tool-makers microscope, or from enlarged photographs of the fracture surfaces.

2.5 Fractography by Electron Microscopy

In addition to the optical fractography, detailed scanning and transmission electron microscopy of the various fracture surfaces was undertaken. Two-stage carbon replication was used for the transmission work. Fracture surfaces corresponding to crack growth at particular stress-intensity levels were selected for examination so as to obtain evidence of changes in the mechanism of fatigue crack growth.

3. EXPERIMENTAL OBSERVATIONS

3.1 Rate of Growth of Fatigue Cracks

Crack-growth rates, determined from at least three specimens from each heat-treatment batch, are shown in Figure 1. The characteristic sigmoidal form of the $\log da/dN$ versus $\log \Delta K$ curve is exhibited for each toughness level or toughness/strength condition.

A notable feature of the curves is that the rate of fatigue-crack growth in the linear region is not significantly influenced by toughness or strength level. The growth rate accelerates as the maximum cyclic stress intensity increases beyond about 0.7 times the respective K_{1C} values; as stress intensity amplitudes decrease below $18 \text{ MPa}\cdot\text{m}^{1/2}$, the curves diverge and the proportionality between $\log da/dN$ and $\log \Delta K$ breaks down. At growth rates less than $5 \times 10^{-5} \text{ mm per cycle}$, a threshold stress-intensity amplitude is approached. Fatigue-cycling was not carried out at growth rates of less than $10^{-5} \text{ mm per cycle}$ but extrapolation suggests that the microstructural

changes which result in differences in toughness, and/or strength, also influence the value of the threshold stress intensity.

3.2 Fractographic Examination

Detailed fractographic examinations were made of fracture surfaces of specimens given heat-treatments A (high toughness), C (low toughness but the same strength properties as A) and D (intermediate toughness and higher strength). Specimens given heat-treatment B (i.e. different in toughness but similar in strength to A and C) did not show sufficient differences in fracture topography from those exhibited for heat-treatment A to warrant the same degree of attention.

Inspections of fracture surfaces were made within zones of the following crack growth rates:

- (a) $da/dN < 2 \times 10^{-5}$ mm/cycle; $K_{max}/K_{1C} \sim 0.15$
- (b) da/dN of 7 to 9×10^{-5} mm/cycle; $K_{max}/K_{1C} \sim 0.25$
- (c) da/dN of 2 to 3×10^{-4} mm/cycle; $K_{max}/K_{1C} \sim 0.3 - 0.4$
- (d) da/dN of 5 to 8×10^{-4} mm/cycle; $K_{max}/K_{1C} \sim 0.5 - 0.6$
- (e) da/dN of 2 to 4×10^{-3} mm/cycle; $K_{max}/K_{1C} \sim 0.7 - 0.8$
- (f) Region of unstable over-load fracture; $K_{max} > K_{1C}$

Typical scanning and transmission electron micrographs of the fracture surfaces at the above rates of crack propagation are shown with the relevant $da/dN/\Delta K$ curve for heat-treatments A, C and D in Figures 2, 3 and 4, respectively.

3.2.1 High-Toughness Steel (Heat Treatment A)

In zone (a) of the high-toughness steel ($K_{1C} \sim 100 \text{ MPa.m}^{1/2}$), where a threshold ΔK is approached, a highly reflective fracture surface was obtained. Scanning microscopy, Figure 2, revealed shallow 'feathery' features similar in appearance to the underlying martensitic structure of the steel. Transmission electron microscopy failed to provide any evidence of fatigue 'striation' markings. The apparent relationship between the fracture surface topography and the underlying microstructure could not be substantiated even with replicas taken from lightly etched fractures.

In zone (b), at the commencement of the linear region of the $\log da/dN - \log \Delta K$ curve, the feathery appearance persisted but the surface was more rumpled with patches of shallow secondary cracking clustered in rows across the direction of crack growth (Fig. 2).

In zone (c), in the centre of the linear region, a 'lumpy' fracture surface was obtained and further indications of parallel rows of shallow secondary cracks, transverse to the growth direction, were noted. Transmission electron microscopy of replicas from this zone revealed clear evidence of striation markings whose spacing approximated to the growth rate of $2-3 \times 10^{-4}$ mm per cycle.

In zone (d), the 'lumpy' fracture surface persisted and the secondary cracks became more widely spaced. Replica studies again revealed the presence of the characteristic fatigue striations. In D6AC martensitic steel, the fatigue striations are discontinuously distributed and are not as clearly defined as those in aluminium alloys.

For zone (e), where the growth rate accelerates as the cyclic stress-intensity amplitude approaches K_{1C} , the fracture mode changes, giving rise to the appearance of ductile 'dimples', indicative of void formation and coalescence. These 'dimples' were especially obvious in the transmission electron microscopy of carbon replicas of the fracture surface, Figure 2. Locally, these features were similar to the markings in the unstable, or overload, zone (f) of the fracture surface.

3.2.2 Low-Toughness Steel (Heat Treatment C)

In zone (a), the fracture surface of the low-toughness material ($K_{1C} = 46 \text{ MPa.m}^{1/2}$), was indistinguishable from that of the high-toughness material for the same zone, (see Fig. 3). In

the linear region, where da/dN ranged from 1 to 2×10^{-4} mm per cycle, striations were prevalent. Above $K_{max} = 30 \text{ MPa}\cdot\text{m}^{1/2}$, i.e. for $K_{max}/K_{1C} > 0.66$, the striations were supplanted by regions having the appearance of cleavage fracture. The relative proportion of this 'cleavage-like' fracture increased as K_{1C} was approached. The overload region exhibited a totally 'cleavage-like' fracture surface, characteristic of this low-toughness D6AC steel¹³.

3.2.3 High Strength, Medium Toughness Steel (Heat Treatment D)

Examination of the fracture surfaces of high-strength, medium-toughness (UTS = 1900 MPa, $K_{1C} = 56 \text{ MPa}\cdot\text{m}^{1/2}$) steel again revealed a highly reflective fracture surface in zone (a), i.e. for slow crack-propagation (see Fig. 4). Features on the fracture surface, both in scanning electron micrographs and at magnifications up to $\times 2500$ in carbon replicas, appeared to be associated with the 'feathery' martensitic structure. However, examination of replicas from etched fracture surfaces at high magnification did not show this relationship.

In the linear zone (c), the 'striation' mechanism predominated and as the K_{max}/K_{1C} ratio exceeded 0.7, evidence of ductile dimpling or void formation increased, interspersed with patches of striation markings. The fracture surface in the overload region consisted entirely of ductile dimples varying from 0.2 to $5.0 \mu\text{m}$ in diameter.

4. DISCUSSION

The rates of fatigue-crack propagation in D6AC steel, heat-treated to different strength and toughness levels, are almost identical for amplitudes of stress intensity between 18 MPa^{1/2} and 70 to 80 percent of the plane-strain fracture toughness. Within this range, the rate of fatigue-crack growth per cycle, da/dN , is proportional to $\Delta K^{2.3 \text{ to } 2.5}$. This observation agrees with similar work reported by Feddersen *et al.*¹⁵ for D6AC steel with $\sigma_y = 1455$ to 1500 MPa, UTS = 1600 – 1650 MPa, and K_{1C} varying between 55 and 105 MPa^{1/2}. They stated that the "toughness level, K_{1C} , is not a variable in fatigue-crack propagation provided K_{max} is substantially (as much as 20 ksi.in^{1/2} [22 MPa^{1/2}]) below K_{1C} for the material." These results, therefore, do not support theories^{16,17} that the rate of fatigue-crack growth is inversely proportional to fracture toughness, K_{1C} .

The increase in yield strength from 1440 to 1510 MPa (4.7 percent) between heat-treatment A and heat-treatment D material is, in the present work, not sufficiently large to enable any conclusions to be drawn regarding the influence of yield strength upon rates of fatigue-crack growth in martensitic steels. However, more comprehensive studies by Richards and Lindley¹², Hahn *et al.*¹⁸, Clark and Bates¹⁹ and Barsom *et al.*²⁰ all indicate that substantial changes in yield strength are not reflected by corresponding variations in rates of fatigue cracking.

Analysis of the fracture surfaces reveals that the crack-growth mechanism which produces striation markings persists over the region where $da/dN \propto \Delta K^m$ and growth is virtually independent of K_{1C} . Moreover, this mechanism is apparently insensitive to the microstructural changes accompanying variations in K_{1C} .¹³ Below about 18 MPa^{1/2}, a fatigue threshold is approached and a change in the appearance of the fracture surface is seen. Crack growth in this region has been described by Cooke *et al.*²¹ as structure-sensitive. However, no direct relationship between the surface topography and the underlying microstructure could be found in the present study.

Above 0.7 K_{1C} , tensile fracture modes (void formation and coalescence or micro-cleavage) are associated with accelerated rates of fatigue-crack growth. Micro-void coalescence was observed in the steel of higher strength and medium toughness (1860–1910 MPa, 58 MPa^{1/2}) and in the steel of high-toughness (100 MPa^{1/2}), 1600–1650 MPa strength level. Facets indicative of micro-cleavage were found in the steel of low-toughness (46 MPa^{1/2}), 1600–1650 MPa strength level. Observations of this kind have also been reported by Donahue *et al.*¹¹ and Richards and Lindley¹².

When the volume of material ahead of a crack is exposed to cyclic-strain 'conditioning' (which for martensitic steels leads to cyclic 'softening' and local flow stresses very much less than the tensile yield values²²), it is clearly inappropriate to apply monotonic tensile properties to theoretical predictions for fatigue-crack growth. Furthermore, the expression devised by Donahue *et al.*¹¹, viz $da/dN = 4A/\pi\sigma_y E [K^2 - K_{th}]$, is applicable, as stated, to a wide range of

materials in which the constant A approximates to $2\sigma_y/E$. The dominant material parameter affecting crack growth is then Young's modulus (E), consistent with the observations reported by Hahn *et al.*¹⁸ and Barsom *et al.*⁶ Thus yield strength, like toughness, bears no clear correlation with fatigue-crack growth, at least not in the central region of the crack growth relationship, i.e. where striation formation and crack extension are not influenced by tensile cracking modes.

The practical significance of the present results and considerations is that, although the resistance to fatigue-crack propagation is unlikely to be improved significantly by optimizing mechanical properties, high toughness materials are to be preferred for service under fatigue conditions. This is not because of any inherent resistance to fatigue-cracking but rather because of the extended range of cyclic stress amplitudes over which da/dN is approximately proportional to ΔK^2 before tensile cracking processes (dependent upon K_{1C}) increase crack growth rates.

5. CONCLUSIONS

1. Fatigue testing, under constant amplitude load cycling, of D6AC steel, having various strength and toughness parameters, yields curves having a three-stage, sigmoidal shape when $\log da/dN$ is plotted against $\log \Delta K$.
2. In the central region of these curves, the rate of fatigue crack-growth da/dN is proportional to $\Delta K^{2.4}$ and independent of fracture toughness, for toughness values ranging from 46 to 100 MPa.m^{1/2} at essentially the same tensile strength.
3. Variations of yield and ultimate strength do not produce any significant change in the rate of fatigue-crack growth in the range where da/dN is proportional to $\Delta K^{2.4}$.
4. In the linear region of the curves, cracking proceeds by a mechanism which gives rise to striation marking upon the fracture surface.
5. At amplitudes above $0.7 K_{1C}$, tensile modes of cracking (void coalescence and micro-cleavage) cause progressively accelerated crack growth as K_{1C} is approached.
6. At amplitudes of stress intensity less than 18 MPa m^{1/2}, threshold values of K are approached. Rates of growth in this region are sensitive to changes in material properties and a different mechanism of growth is indicated by a change in fracture surface topography.

REFERENCES

1. Paris, P. C., and Erdogan, F., Trans. ASME, **85**, 1963, 528.
2. Brothers, A. J., and Yukawa, S., *ibid*, **89**, 1967, 19.
3. Miller, G. A., Trans. ASM, **61**, 1968, 442.
4. Clark, W. G., and Trout, H. E., J. Eng. Fracture Mech., **2**, 1970, 107.
5. Actil, A. A., and Kula, E. B., ASTM. STP. 462, 1971, 297.
6. Barsom, J. M., Trans. ASME, **93B**, 1971, 1190.
7. Pelloux, R. M., Proc. USAF. Conf. on Fatigue of Aircraft Structures and Materials. AFFDL: TR.-70-144, 1970, pp. 409.
8. Schwalbe, K. H., J. Eng. Fracture Mech., **6**, 1974, 325.
9. Liu, H. W., Appl. Mat. Res. **7**, 1964, 229.
10. Crooker, T. W., and Lange, E. A., U.S. Naval Res. Lab. Rept. N.R.L. 6944, 1969.
11. Donahue, R. J., Clark, H. McL., Atanmo, P., Kumble, R., and McEvily, A. J., Int. J. Fract. Mech., **8**, 1972, 209.
12. Richards, C. E., and Lindley, T. C., J. Eng. Fracture Mech. **4**, 1972, 951.
13. Ryan, N. E., Aero. Research Labs, Met. Note 103, 1974.
14. Peterman, G. L., and Jones, R. L., Metals Eng. Q'ly, **2**, 1975, 15.
15. Fedderson, G. E., Moon, D. P., and Hyler, W. S., Crack Behaviour in D6AC Steel, Metals and Ceramics Information Centre, MCIC, 72-04, 1972.
16. Krafft, J. M., ASM. Trans. Q'ly, **58**, 1965, 691.
17. Rice, J. R., ASTM. STP 415, 1967, 247.
18. Hahn, G. T., Sarrate, M., and Rosenfield, A. R., Proc. USAF. Conf. on Fatigue of Aircraft Structures and Materials. AFFDL: TR 70-144, 1970, 425.
19. Clark, W. G., and Bates, R. C., Trans. ASM., **62**, 1969, 380.
20. Barsom, J. M., Imhof, E. J., and Rolfe, S. T., J. Eng. Fracture Mech. **2**, 1971, 301.
21. Cooke, R. J., Irving, P. E., Booth, C. S. and Beevers, C. J., J. Eng. Fracture Mechanics, **7**, 1975, 69.
22. Landgraf, R. W., Morrow, J. and Endo, J., J. of Materials, **4**, 1969, 176.

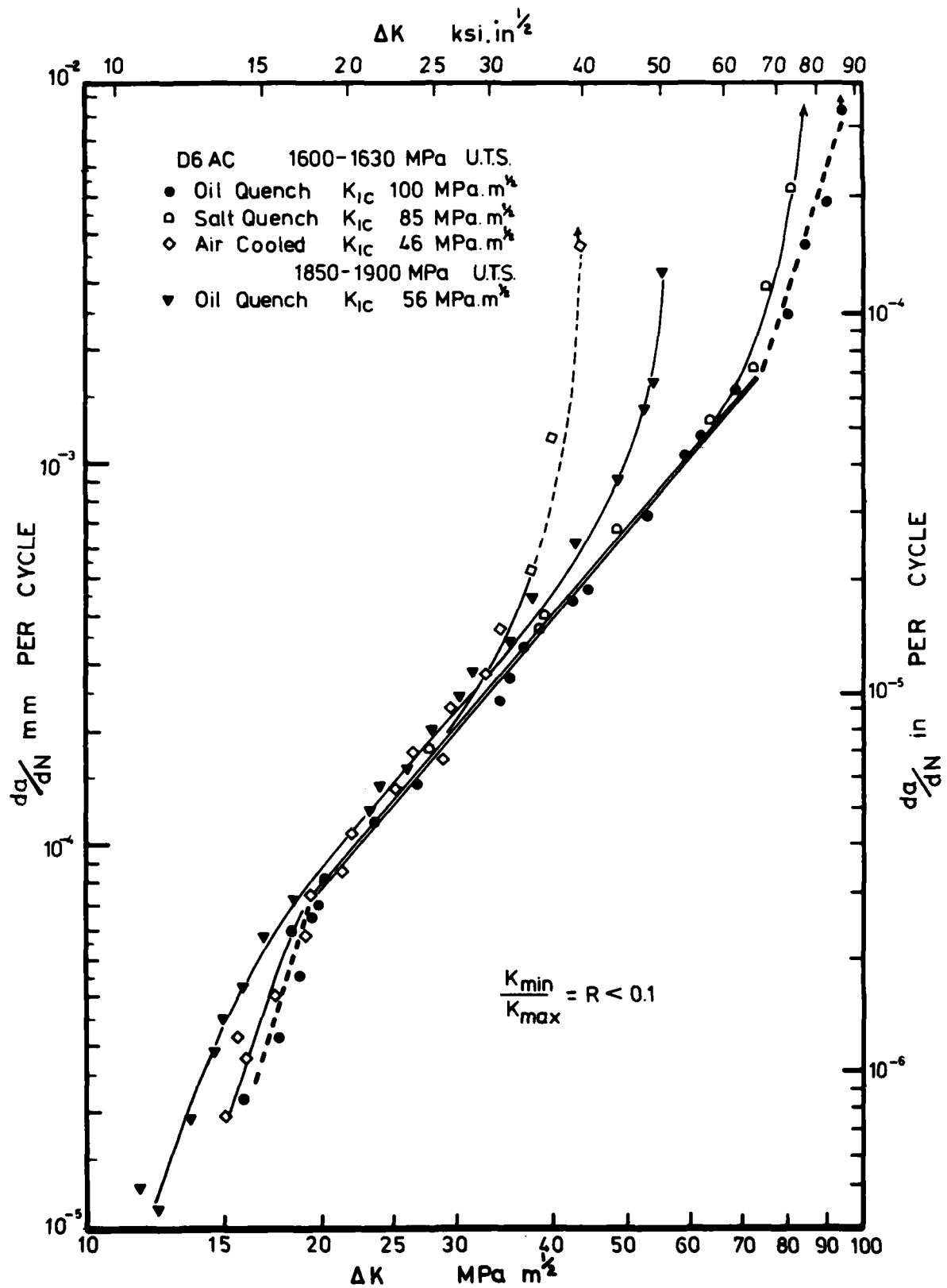


Fig. 1. Rates of fatigue – crack growth, da/dN , in D6AC steel, heat treated to different strength and toughness (K_{Ic}) values, as a function of stress – intensity amplitudes, ΔK .

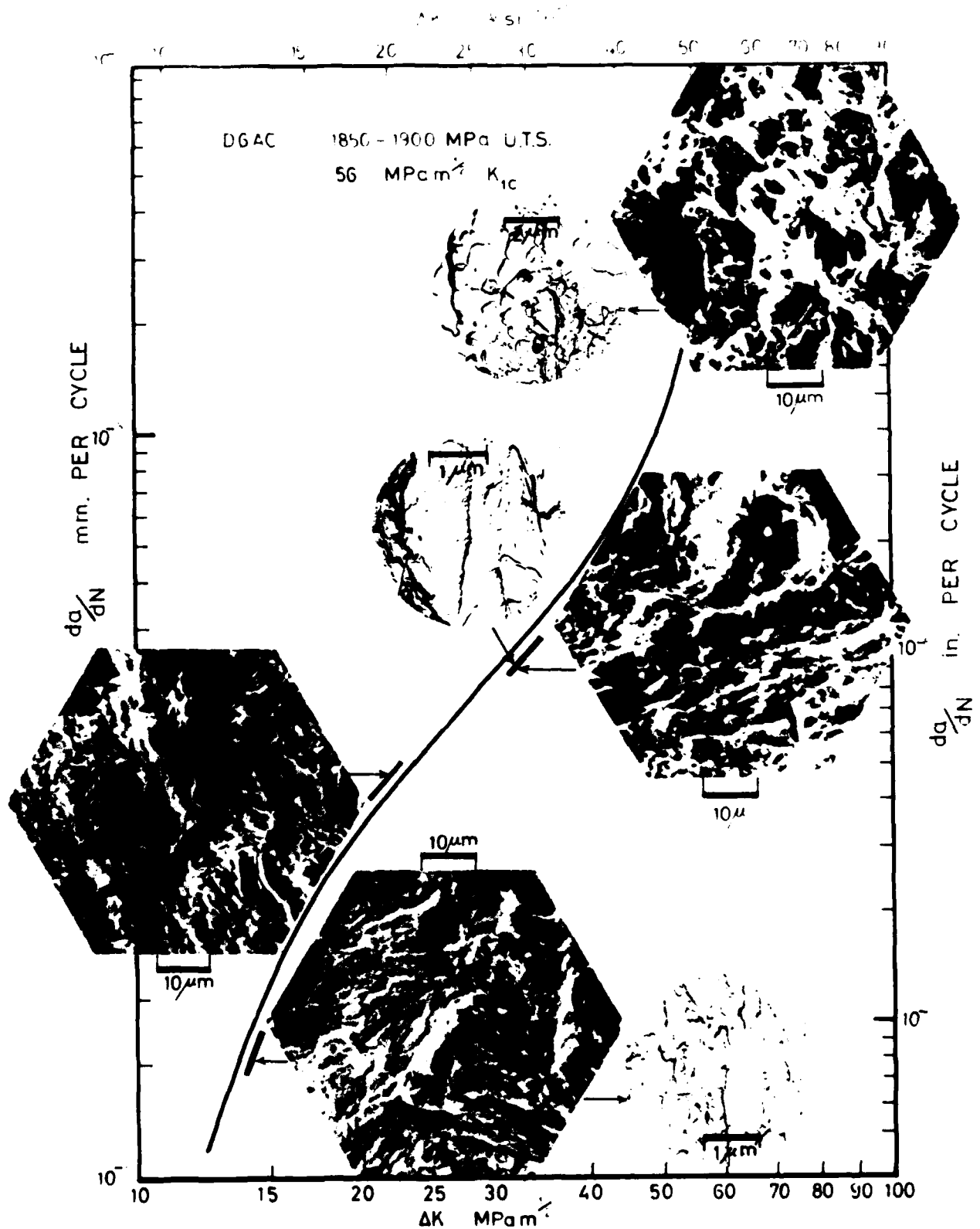


Fig. 4. Fractographic features exhibited on the fatigue-fracture surface of DGAC steel, heat treated to U.T.S. = 1850 - 1900 MPa, K_{1c} = 56 MPa m^{1/2} (heat treatment D). Hexagonal photographs are SEM fractographs; circular photographs are TEM fractographs using germanium - shadowed carbon replicas.

DISTRIBUTION

AUSTRALIA

Copy No.

Department of Defence

Central Office

Chief Defence Scientist	1
Deputy Chief Defence Scientist	2
Superintendent, Science and Technology Programs	3
Australian Defence Scientific and Technical Representative (U.K.)	5
Counselor, Defence Science (U.S.)	6
Defence Library	7
Joint Intelligence Organisation	8
Assistant Secretary, D.I.S.B.	9-24

Aeronautical Research Laboratories

Chief Superintendent	25
Superintendent, Materials Division	26
Materials Divisional File	27
Author: N. E. Ryan	29
Library	30
Superintendent, Structures Division	31
CAARC Structures Coordinators, per Dr F. H. Hooke	32-37
Dr A. O. Payne	38
B. C. Hoskin	39
J. Y. Mann	40
G. S. Jost	41

Material Research Laboratories

Library	42
---------	----

Defence Research Centre, Salisbury

Library	43
---------	----

Engineering Development Establishment

Library	44
---------	----

RAN Research Laboratory

Library	45
---------	----

Navy Office

Naval Scientific Adviser	46
--------------------------	----

Army Office

Army Scientific Adviser	47
Royal Military College Library	48
US Army Standardisation Group	49

Air Force Office

Air Force Scientific Adviser	50
Aircraft Research and Development Unit	51
Engineering (CAFTS) Library	52
D. Air Eng.	53
HQ Support Command (SENGSO)	54
RAAF Academy, Point Cook	55

Department of Productivity		
Government Aircraft Factories		
Library		56
Department of Transport		
Secretary, Library		57
Airworthiness Group (Mr R. Ferrari)		58
Statutory, State Authorities and Industry		
Australian Atomic Energy Commission, Director		59
C.S.I.R.O. Materials Science Division, Director		60
Qantas, Library		61
Trans Australia Airlines, Library		62
Gas and Fuel Corporation of Victoria, Research Director		63
SEC of Victoria, Herman Research Laboratory, Librarian		64
SEC of Queensland, Library		65
Ansett Airlines of Australia, Library		66
Australian Paper Manufacturers, Dr Norman		67
BHP Central Research Laboratories, NSW		68
BHP Melbourne Research Laboratories		69
Commonwealth Aircraft Corporation:		
Manager		70
Manager of Engineering		71
Victorian Brown Coal Council, Dr Worner		72
Hawker de Havilland Pty Ltd:		
Librarian, Bankstown		73
Manager, Lidcombe		74
ICI Australia Ltd, Library		75
Rolls Royce of Australia Pty Ltd, Mr Mosley		76
Universities and Colleges		
Adelaide	Barr Smith Library	77
Australian National	Library	78
Flinders	Library	79
James Cook	Library	80
La Trobe	Library	81
Melbourne	Engineering Library	82
Monash	Library	83
	Professor I. J. Polmear	84
	Dr J. Griffiths	85
Newcastle	Library	86
New England	Library	87
New South Wales	Physical Sciences Library	88
Queensland	Library	89
	Metallurgy Department	90
Sydney	Professor G. A. Bird	91
Tasmania	Engineering Library	92
Western Australia	Library	93
R.M.I.T.	Library	94
	Head of Engineering Department (N. Herbst)	95
CANADA		
Aluminium Laboratories Ltd, Library		96
CAARC Coordinator Structures		97
Physics and Metallurgy Research Laboratories, Dr A. Williams		98
National Aeronautical Establishment, (NRC) Library		99

Universities and Colleges		
McGill	Library	100
Toronto Institute for Aerospace Studies		101
FRANCE		
AGARD, Library		102
ONERA, Library		103
Service de Documentation, Technique de l'Aeronautique		104
GERMANY		
ZLDI		105
INDIA		
CAARC Coordinator Materials		106
Civil Aviation Department, Director		107
Defence Ministry, Aero Development Establishment, Library		108
Hindustan Aeronautics Ltd, Library		109
Indian Institute of Science, Library		110
Indian Institute of Technology, Library		111
National Aeronautical Laboratory, Director		112
ISRAEL		
Technion—Israel Institute of Technology, Professor J. Singer		113
ITALY		
Associazione Italiana di Aeronautica e Astronautica, Professor A. Evla		114
JAPAN		
National Aerospace Laboratory, Library		115
Universities		
Tohoku (Sendai)	Library	116
	T. Yokobori	117
Tokyo	Institute of Space and Aeroscience	118
NETHERLANDS		
Central Organization for Applied Science Research TNO, Library		119
National Aerospace Laboratory (NLR) Library		120
National Aerospace Institute, Dr J. Schijve		121
University		
Delft	Dr D. Broek	122
NEW ZEALAND		
Air Department, R.N.Z.A.F. Aero Documents Section		123
Transport Ministry, Civil Aviation Division, Library		124
Universities		
Canterbury	Library	125
	Professor D. Stevenson, Mechanical Eng.	126
	Mr F. Fahy, Mechanical Engineering	127
	Mr J. Stott, Chemical Engineering	128
Auckland	Professor A. L. Tichener	129
SWEDEN		
Aeronautical Research Institute		130
Chalmers Institute of Technology, Library		131
Kungliga Tekniska Hogskolan		132

SAAB-Scania, Library	133
Research Institute of the Swedish National Defence	134

SWITZERLAND

Armament Technology and Procurement Group	135
Brown Boverie, Management Chairman	136
Escher-Wyss Ltd, Manager	137

UNITED KINGDOM

Mr A. R. G. Brown, ADR/Mat (MEA)	138	
Aeronautical Research Council, Secretary	139	
C.A.A.R.C., Secretary	140	
Royal Aircraft Establishment:		
Farnborough, Library	141	
Bedford, Library	142	
Royal Armament Research and Development Establishment	143	
Commonwealth Air Transport Council Secretariat	144	
Aircraft and Armament Experimental Establishment	145	
Military Vehicles Engineering Establishment	146	
Admiralty Materials Laboratories, Dr R. G. Watson	147	
National Engineering Laboratories, Superintendent	148	
National Gas Turbine Establishment, Director	149	
National Physical Laboratories, Library	150	
British Library, Science Reference Library	151	
British Library, Lending Division	152	
Naval Construction Research Establishment, Superintendent	153	
Aircraft Research Association, Library	154	
British Ship Research Association	155	
C. A. Parsons, Gas Turbine Dept., Library	156	
Central Electricity Generating Board, Dr C. Richard:	157	
Fulmer Research Institute Ltd, Research Director	158	
Science Museum Library	159	
Welding Institute, Library	160	
Hawker Siddeley Aviation Ltd:		
Brough, Library	161	
Greengate, Library	162	
Kingston-upon-Thames, Library	163	
Hawker Siddeley Dynamics Ltd, Hatfield	164	
British Aircraft Corporation [Holdings] Ltd:		
Commercial Aircraft Division	165	
Military Aircraft Division	166	
British Hovercraft Corporation Ltd, Library	167	
Fairey Engineering Ltd, Hydraulic Division	168	
Short Brothers Harland	169	
Westland Helicopters Ltd	170	
Universities and Colleges		
Bristol	Library, Engineering Department	171
Cambridge	Library, Engineering Department	172
	Professor Honeycombe, Metallurgy	173
	Dr Knott, Metallurgy	174
London	Professor A. D. Young, Aero Engineering	175
Manchester	Professor E. Smith	176
Nottingham	Library	177
Sheffield	Professor G. Greenwood, Metallurgy	178
	Dr S. J. Maddox, Department of Mech. Eng.	179

Southampton	Library	180
Strathclyde	Library	181
Cranfield Institute of Technology	Library	182
Imperial College	The Head	183

UNITED STATES OF AMERICA

Aerospace Corporation:		
Dr L. Raymond		184
Dr E. G. Kendall		185
General Dynamics Corporation		186
N.A.S.A. Langley Research Centre:		
H. F. Hardrath		187
C. M. Hudson		188
N.A.S.A. Scientific and Technical Information Facility		189
Scania Group Research Organisation		190
American Institute of Aeronautics and Astronautics		191
Applied Mechanics Reviews		192
The John Crerar Library		193
The Chemical Abstracts Service		194
Allis Chalmers Inc., Director		195
Boeing Company:		
Head Office, Mr R. Watson		196
Industrial Production Division		197
Lockheed Missiles and Space Company		198
Lockheed California Company		199
Lockheed Georgia Company		200
McDonnell Douglas Corporation, Director		201
Metals Abstracts, Editor		202
United Technologies Corporation, Pratt and Whitney Aircraft Group		203
Battelle Memorial Institute, Dr G. T. Hahn		204
Calspan Corporation, Professor H. Johnson		205
Rockwell International, Dr H. L. Marcus		206
U.S. Steel Applied Research Labs, J. M. Barsom		207
U.S. Naval Research Labs:		
T. W. Crooker		208
C. D. Beachum		209
General Dynamics Corporation		210
Universities and Colleges		
Brown	Professor J. R. Rice	211
California	Professor A. S. Tetelman	212
Carnegie-Mellon	Professor J. L. Swedlow	213
Connecticut	Professor A. J. McEvily	214
Florida	Library, Documents Department	215
	Mark H. Clarkson, Dept of Aero Eng.	216
Harvard	Professor A. F. Carrier, Applied Mathematics	217
	Dr S. Goldstein	218
Johns Hopkins	Professor S. Corrain	219
Lehigh	Professor G. C. Gih	220
	Professor R. P. Wei	221
Stanford	Library, Department of Materials Science	222
Wisconsin	Memorial Library, Serials Department	223
Brooklyn Institute of Polytechny	Library, Polytech Aeronautical Labs	224

California Institute		
of Technology	Guggenheim Aeronautical Labs	225
Massachusetts Institute of Technology:	N. J. Grant	226
	R. M. Pelloux	227

Spares		228-237
--------	--	---------

END

DATE
FILMED

8-80

DTIC